Electronic Supplementary Material (ESI) for Physical Chemistry Chemical Physics.
This journal is © the Owner Societies 2019

Modulating and probing the dynamic intermolecular interactions in plasmonic molecule-pair junctions

Tao Ma,[1,2] Jing Guo,[2] Shuai Chang,[1,3*] Xuewen Wang,[2] Jianghao Zhou,[2,3] Feng Liang,[1*] Jin He[2,4*]

[1] The State Key Laboratory of Refractories and Metallurgy, School of Chemistry and Chemical Engineering, Wuhan University of Science and Technology, Wuhan 430081, China
[2]Department of Physics, Florida International University, Miami, Florida 33199, USA
[3]School of Materials and Metallurgy, Wuhan University of Science and Technology, Wuhan 430081, China
[4]Biomolecular Science Institute, Florida International University, Miami, Florida 33199, USA

*E-mail: Schang23@wust.edu.cn, feng_liang@whu.edu.cn, jinhe@fiu.edu

Table of content

S1. GNE surface modification and characterization, and junction molecule number estimation.

The full details of GNE fabrication, characterization and chemical modification can be find in the supporting information of a previous report.[1] Before and after 4-MBA modification of GNE, we acquired cyclic voltammograms (CVs) of the same GNE. For comparison, we also tested thiol phenol (TP) molecule. As shown in Figure S1 a and b, the current above +0.4 V is clearly saturated, which is diffusion-limited. The magnitude of the diffusion-limited current is proportional to the effective area of GNE NOT covered by molecules. The saturation current decrease is about 82.7% for the 4-MBA modified GNE and is about 5.78% for TP modified GNE. Therefore, the surface coverage of 4-MBA is much lower than TP. It has been revealed from Raman studies that TP is almost normal to the gold surface but the 4-MBA tilted about 33 degree to the normal axis because of the carboxyl group.[2] The tilted 4-MBA occupies a bigger foot-print and thus reduce its surface coverage.

Figure S1c shows a typical SEM image of a 4-MBA modified GNE with adsorbed GNPs. Only two GNPs are visible on the GNE apex. The adsorbed GNP forms a GNP/molecule/GNE geometry. To estimate the number of molecule or molecule pair in the junction, we need to consider the cross-section area of the 'hot spot' in the nanogap. Based on FDTD calculation of the GNP/molecule/GNE geometry, the cross-section radius r for the 'hot spot' region with electromagnetic enhancement factor (EF)>10^9 is about 3.15 nm when the GNE (with radius R_1= 150 nm) and GNP (with radius R_2=20 nm) gap distance is 0.9 nm (about the length of one 4-MBA molecule). The hotspot size will be even smaller when the gap distance is bigger for a 4-MBA/4MBA pair. The cross-section area of 'hot spot' is $A=\pi r^2=31$ nm^2 and the estimated molecule number in the hot spot is around 46 molecules.

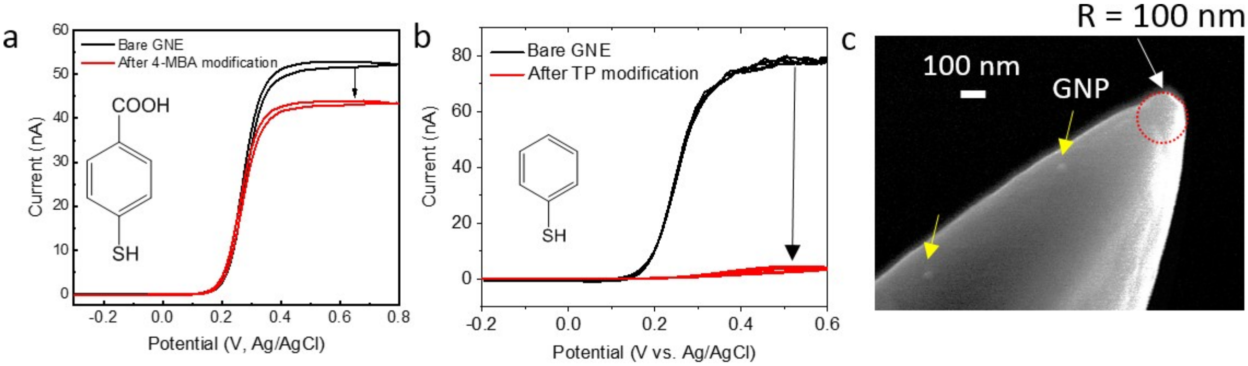

Figure S1 (a-b) The CVs of GNE before and after the surface modification with 4-MBA (a) and TP (b) respectively. The cleaned GNEs are immersed in molecule (50 mM for both 4-MBA and TP) ethanol solution for overnight to achieve a stable SAM at the GNE apex. The CVs were measured in 1M KCl with 100 mM $K_4Fe(CN)_6$ and the sweep rate is 50 mV/s. (c) The SEM image of a GNE modified with 4-MBA. The tip radius is about 100 nm.

S2. DFT calculations of Raman spectra and peak assignment

We have performed B3LYP functional based DFT calculations using Gaussian 09 package. Although B3LYP is the most widely used functional, the B3LYP functional based DFT calculations has its limitations in calculating long-range noncovalent interactions, such as London dispersion forces,[3, 4] which affecting the accuracy of the DFT calculations of molecule-pair. However, it can still provide insightful view at the atomic level.

Figure S2a shows the optimized molecular structures of molecule-pair junctions (1 and 2) with intermolecular h-bonds (indicated by white color dash lines). The h-bond distance at equilibrium in gas phase is unrealistically short (less than 0.2 nm). However, by changing the distance of two fixed gold atoms, the h-bond length and strength can be altered. In this way, we can probe how the spectra changes with the h-bonds between two molecules.

Figure S2b shows the calculated Raman spectra of different types of junctions. The two major a1 symmetric modes 7a and 8a are pronounced in all the spectra. Figures S2 c and d show the zoomed in region marked in Figure S2a. In Figure S2c, the peak near 1000 cm^{-1} is due to the in-plane asymmetric ring breathing mode (b2). In the symmetric 4-MBA/4MBA junction, this peak is from the overlapped contributions of both benzene rings. However, this peak splits to two in asymmetric 4-ATP/4-MBA junction. We did not observe the simultaneous appearance of two peaks near 1003 and 1027 cm^{-1} in the calculations. In experiments, the two peaks always appear together and both peaks are assigned to the in-plane asymmetric breathing modes. The charge redistribution/transfer and the mechanical deformation of molecular structure during interaction are suggested to play important roles for the appearance of double peaks, which will be tested in future calculations.

The peak appears in Figure S2d is due to the *v*(C=O) vibrational mode of 4-MBA carboxyl group. The peak of *v*(C=O) mode shifts significantly to the lower wavenumber (red shift) in both molecule-pair junctions, attributing to the intermolecular h-bonds. The red shift is bigger for 4-MBA/4-MBA, suggesting the h-bonds between two 4-MBA molecules are stronger. As shown in Figure 2e, we also find the *v*(C=O) peak red-shifts more (the C=O bond is weaker) when the h-bond is stronger (shorter bond distance) between two 4-MBA molecules.

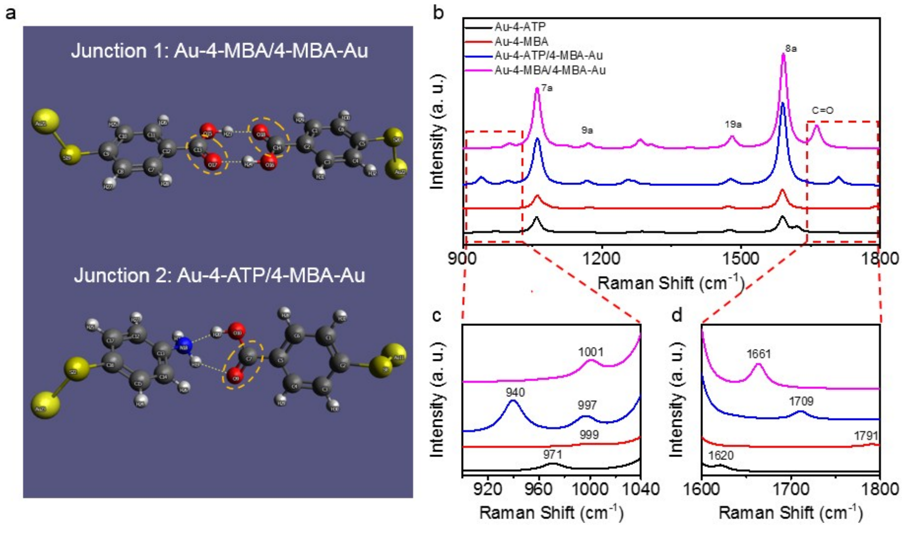

Figure S2. (a) The molecular structures of junction 1 (top) and junction 2 (bottom). (b) The DFT calculated spectra of Au-4-ATP, Au-4-MBA, Au-4-ATP/4-MBA-Au and Au-4-MBA/4-MBA-Au, and their detail views in dotted square (c) and (d).

Based on DFT calculations and previous reports, the assignments of vibrational modes for 4-MBA and 4-ATP in the range 1000 -1800 cm^{-1} are summarized in Table S1. The normal Raman are collected from molecule powders. For ring vibrations, the symmetry is assigned based on C_{2v} symmetry. To avoid confusion, here we follow the same assignment of 4-ATP molecule for 4-MBA molecule. The actual peak position might vary by several wavenumbers owing to small changes of local environment and experimental conditions.

Table S1. Raman peak assignment of 4-MBA and 4-ATP (1000 cm^{-1} to 1800 cm^{-1}).

4-MBA peak (cm^{-1})				4-ATP peak (cm^{-1})			
SERS GNE-4-MBA/GNP	DFT Raman	Normal Raman (powder)	Assignment[5-8]	SERS GNE-4-ATP/GNP	DFT Raman	Normal Raman (powder)	Assignment[9]
1003	999	-	Ring breathing, b2	1008	971	1011	18a, Ring breathing
1027	-	-	Ring breathing, b2				
1080	1058	1098	7a, $\nu(CC)_{ring} + \nu(C\text{-}S)$	1081	1061	1089	7a, $\nu\ (CC)_{ring} + \nu(C\text{-}S)$
1185	1173	1180	9a, δ(CH)	1192		1173	9a, δ(CH)
1382	-	-	$\nu(COO^-)$				
1486	1474	1453	19a, ν(CC) + δ(CH)	1483	1475	1490	19a, ν(CC) +δ(CH)
1582	-	-	8b, $\nu(CC)_{ring}$	1584			8b, $\nu(CC)_{ring}$
1593	1590	1600	8a, $\nu(CC)_{ring}$	1594	1590	1595	8a, $\nu(CC)_{ring}$
1710	1785	1620	ν(C=O)				

The notations of the modes are: ν = stretching; β = in-plane bending; δ = in-plane deformation. γ = out-of-plane deformation

S3. Raman spectra of different types of junctions during 'hit-stay-run' collision events

The SERS spectral changes induced by GNP 'hit-stay-run' collision events are observed in different types of junctions. Figure S3 shows the typical SERS time traces in heat map for junctions containing 4-MBA/4-MBA molecule-pair (a), 4-ATP (b), and 4-MBA (c) with GNPs in the solution at zero bias. These traces are collected at the very early stage of the experiments after adding GNPs in the solution (3mM $K_4Fe(CN)_6$ + 5 mM PBS). The black spectra shown at the bottom panel are the baseline spectra, which are from the adsorbed GNPs on the GNE. The baseline intensity increase speed reflects the interaction strength and we can conclude that the interaction strength follows this sequence: 4-ATP/Au > 4-MBA/4-MBA > 4-MBA/Au.

The collision events (indicated by the red arrows) often appear as bight lines in SERS heat map. The reason is that the collision events lead to the formation of hotspots, inducing uniform enhancement of the baseline intensity. The red color spectra shown at the bottom panel are the typical transient spectra during these ‘hit-stay-run’ events.

We also compared the spectra collected at 0.5 V. Figures S3 a and b show typical SERS results for junctions containing 4-ATP/4-MBA and 4-MBA/4-MBA molecule-pairs. These spectra are the same as the ones at zero bias. However, the collision event rates are obviously higher at + 0.5 V, as shown in Figure S2c. Between 4-ATP/4-MBA and 4-MBA/4-MBA pairs, the event rate for 4-MBA/4-MBA experiment is always lower, which is attributed to the electrostatic repulsive-force between two carboxyl groups. In addition, the baseline intensity of 4-ATP/4-MBA spectra also increased faster after adding GNPs in the solution.

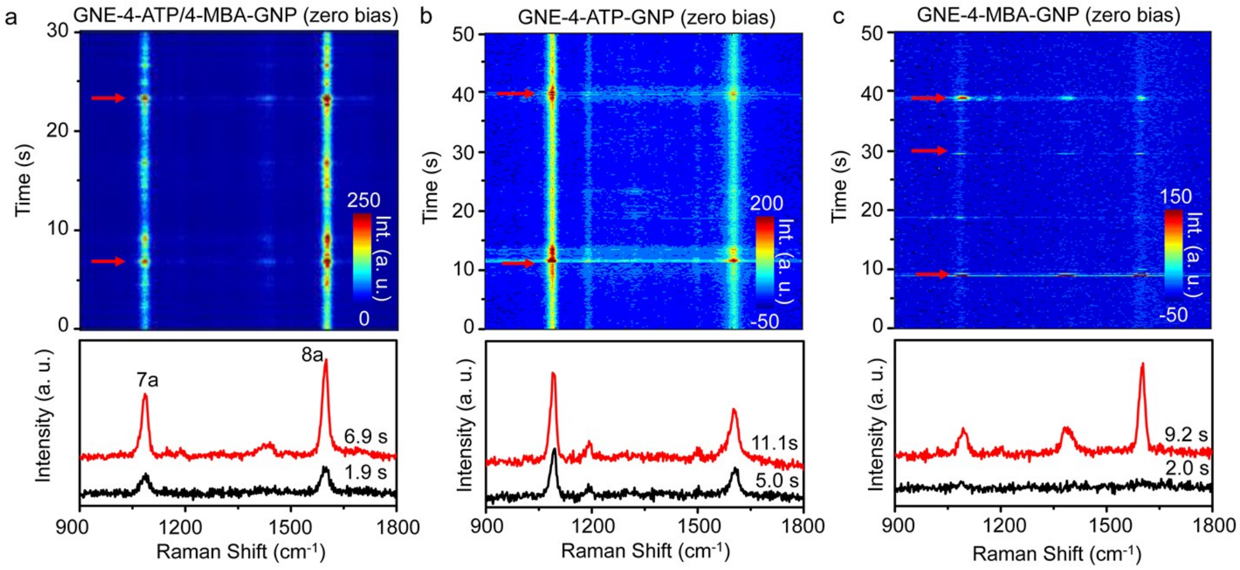

Figure S3. (a-c) The time-resolved SERS trajectory in heat map (top panel) and transient spectra (bottom panel) of junctions: (a) GNE-4-ATP/4-MBA-GNP, (b) GNE-4-ATP-GNP, and (c) GNE-4-MBA-GNP. The “hit-stay-run” collision events are indicated by red color arrows in heat map. The experiments are carried out at zero bias in 3mM $K_4Fe(CN)_6$ + 5 mM PBS solution with 30 pM GNP.

All the transient spectra during collision have two pronounced peaks near 1083 cm^{-1} and 1592 cm^{-1}. In addition, two small peaks often appear and are more noticeable during these collision events than in the stable junctions by adsorbed GNPs (see Figure S3). They are likely excited by the collision events. For the transient GNP-4-MBA-GNE junction, we often observe a small peak near 1380 cm^{-1}. This peak is attributed to *v*(COO$^-$) of the carboxyl group. For the transient GNP-4-MBA/4-MBA-GNE junction, we often observe two small peaks. One peak is near 1425 cm^{-1} and the other is near 1700 cm^{-1}, which are assigned to *v*(COO$^-$) and *v*(C=O) modes of carboxyl group, respectively. Compared with the 4-MBA junction, the *v*(COO$^-$) peak position here is red-shifted significantly. These spectral changes are all related to the carboxyl group, which is easier to be affected during the collision events.

In electrolyte, we never observe the 1003 cm^{-1} and 1027 cm^{-1} peaks in the transient spectra of all the junctions during hit-stay-run events. However, both peaks can be observed sometimes when the solution is changed to DI water. This is expected because the intermolecular interactions are stronger in DI water with reduced charge screening.

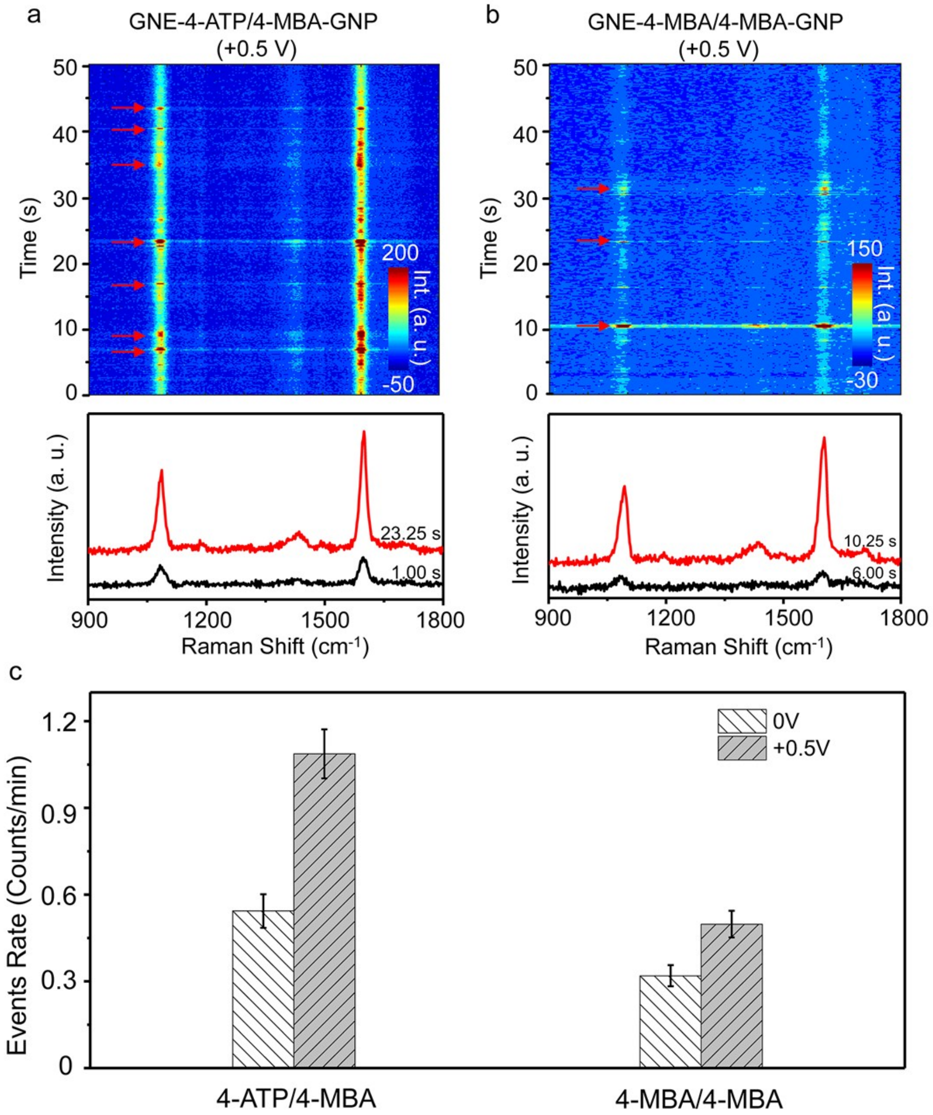

Figure S4. (a-b) The time-resolved SERS trajectory in heat map (top panel) and transient spectra (bottom panel) of junctions GNE-4-ATP/4-MBA-GNP (a) and GNE-4-ATP/4-MBA-GNP (b). The "hit-stay-run" collision events are indicated by red color arrows in the heat map. The experiments are carried out at + 0.5 V bias in 3 mM $K_4Fe(CN)_6$ + 5 mM PBS solution with 30 pM GNP. (c) The event rates of "hit-stay-run" events for GNE-4-ATP/4-MBA-GNP and GNE-4-MBA/4-MBA-GNP experiments in first 10 minutes after adding 4-MBA modified GNPs in solution at zero and 0.5 V bias. The error bars are the standard deviation of three repetitive experiments.

Figure S5 show the dynamic spectral changes when a 4-MBA modified GNP lands and stays on a 4-ATP modified GNE. The development of chemical interactions in 4-ATP/4-MBA pair junction is revealed. The results are similar to Figures 1 c-e in main text. However, the higher intensity of

1003 cm^{-1} and 1028 cm^{-1} peaks and the bigger red-shift of 8a suggest the stronger intermolecular interactions between 4-MBA and 4-ATP, which is attributed to the attractive electrostatic forces between amine and carboxyl groups. The dependence of these spectral changes on solution salt concentration and the interaction partner suggests the origin of these changes are from intermolecular interactions.

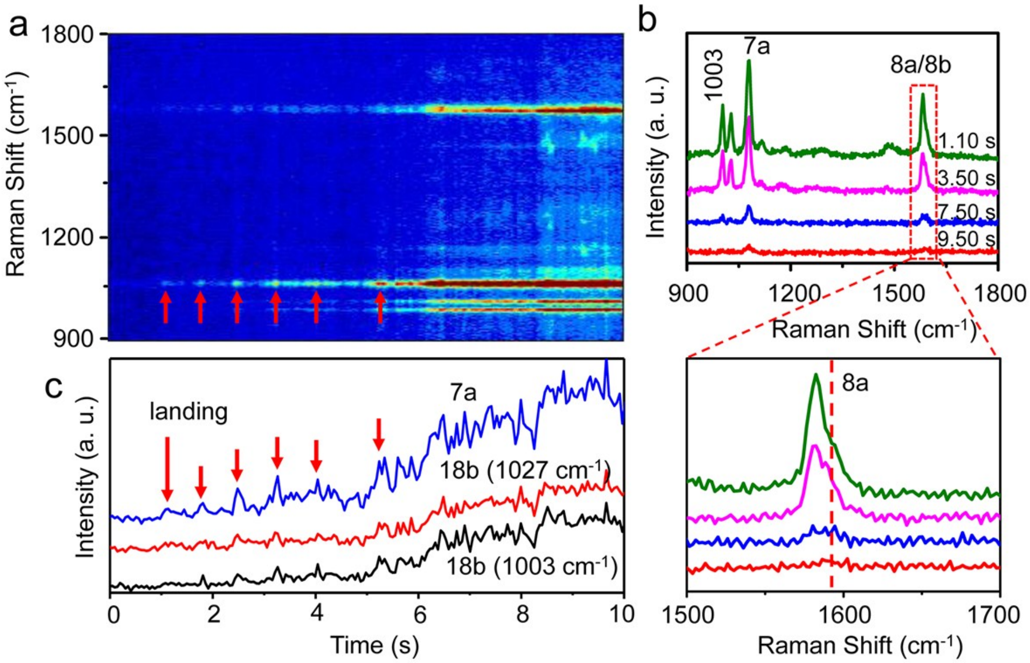

Figure S5. (a) A typical time-resolved SERS heat map trajectory showing the spectral changes of 4-ATP/4-MBA junction induced by a 'hit-n-stay' event in electrolyte. (b) Four spectra appeared sequentially in trajectory (c). The zoom-in spectra at the bottom show the spectral red-shift of mode 8a. (c) The intensity-time traces of 1083 cm^{-1} (7a), 1003 cm^{-1} and 1027 cm^{-1}. The results are displayed with an offset for clarity. All the results are collected with the GNE at zero bias at room temperature. The electrolyte is 5 mM PBS with pH 7.4, containing 3 mM Potassium Ferrocyanide and 30 pM 40 nm GNPs.

S4. The Dynamics of H-Bonds in Established 4-ATP/4-MBA Junctions

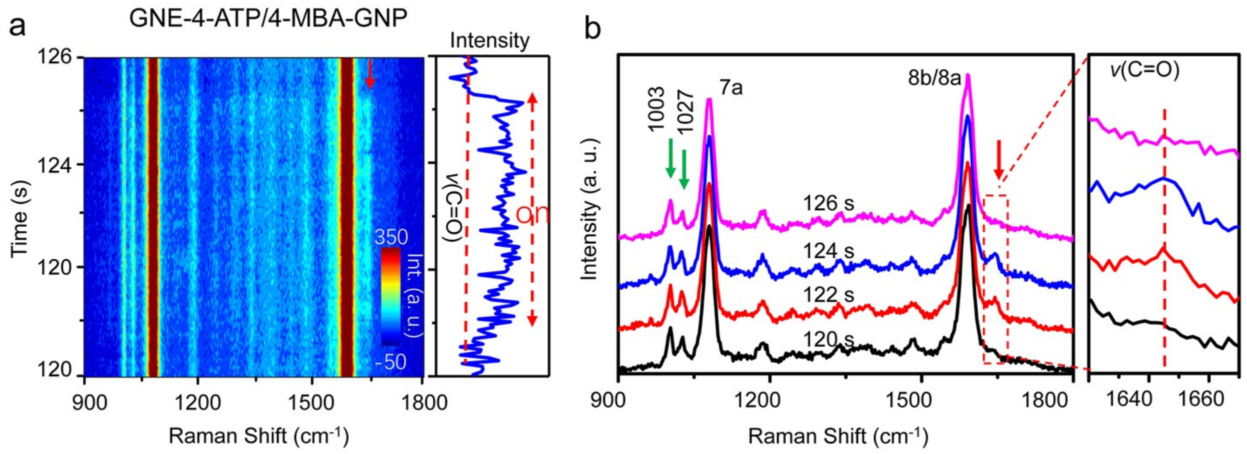

Figure S6. (a) Left: representative SERS heat map trajectory of GNE-4-ATP/4-MBA-GNP junction showing sudden appearance of *v*(C=O) mode at 1651 cm^{-1}. Right: the intensity-time trace of *v*(C=O) mode. (b) Four progressive spectra selected from (a). The zoom-in spectra at the right magnify the changes of *v*(C=O) mode. The spectra offset vertically. All the experiments were conducted at zero bias and the electrolyte containing no GNPs.

Different from the results of 4-MBA/4-MBA junction in Figure 2, only a new peak of *v*(C=O) around 1645 cm^{-1} appears transiently between 121 s and 125 s in the trajectory. The peak of *v*(COO-) mode is not observed.

S5. Stable SERS spectra of established GNE-4-MBA/GNP junctions.

After adding GNPs in the solution for some time, the baseline intensity is gradually stabilized. Although spectral fluctuations still happen from time to time, the spectra are generally stable. At this time, one or a few GNPs stay at the GNP apex by chemical interactions. We then replace new solution to remove free GNPs in the solution. Figure S7a shows the typical stable SERS spectra measured in established GNE-4-MBA/GNP junctions after the permanent adsorption of GNP ('hit-n-stay'). The 1003 cm^{-1} and 1027 cm^{-1} peaks are stable in the spectrum. The appearance of both peaks is attributed to the charge transfer between carboxyl group and the under-coordinated gold atoms at the molecule-metal interface, which modifying the molecule electronic structure and reducing the electron intensity in the benzene ring.

Figure S7b shows the pH dependence of *v*(COO-) and *v*(C=O) modes of 4-MBA in stable GNE-4-MBA/GNP molecular junctions. The *v*(COO$^-$) mode is only observed in alkaline solution (high pH) due to deprotonated 4-MBA, while the *v*(C=O) mode is only observed in acidic solution (low pH). The two modes do not appear at the same time. This is consistent with previous report.[10]

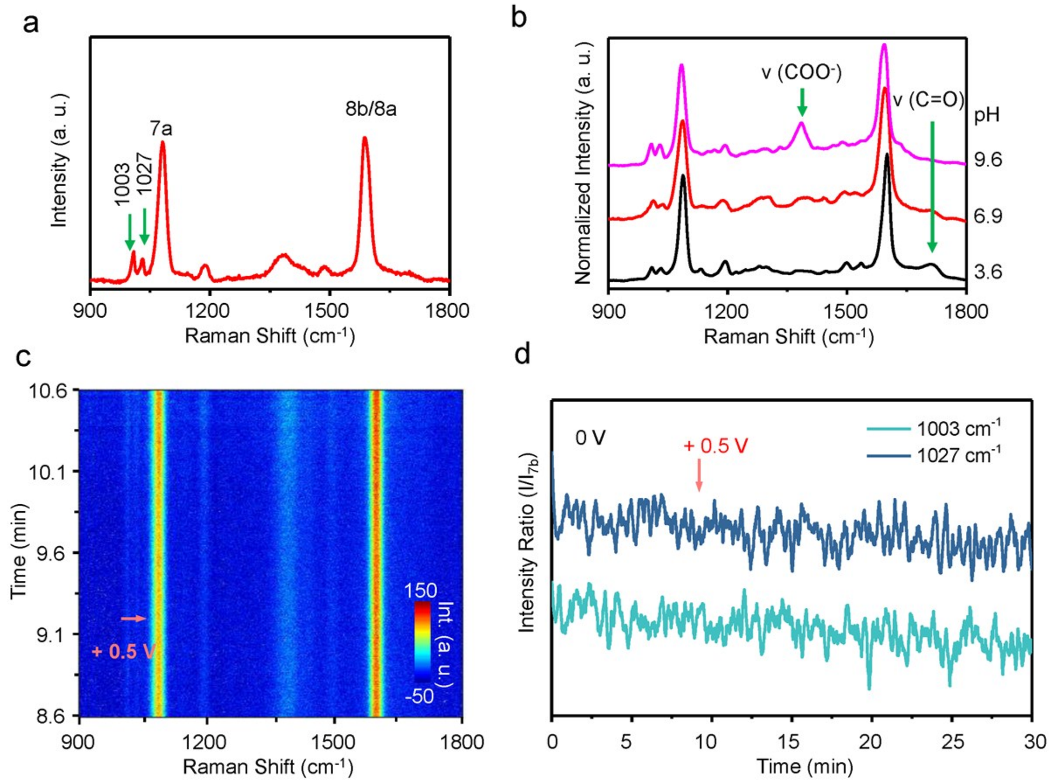

Figure S7. (a) The typical SERS spectrum of stable GNE-4-MBA/GNP junction at pH=7. (b) The SERS spectra of GNE-4-MBA/GNP in 10 mM KCl solution with pH at 3.6 (black color curve), 6.9 (red color curve), and 9.6 (magenta color curve), respectively. For above results, no bias was applied at the GNE and no GNP. (c) A time-resolved SERS trajectory to show the intensity and spectral changes after applying +0.5 V. (d) The intensity (I/I_{7a})-time traces of modes 1003 cm^{-1} and 1027 cm^{-1}. All the experiments are conducted in the solution with 3mM $K_4Fe(CN)_6$ and 5 mM PBS.

S6. Appearance time of h-bonds in established 4-MBA/4-MBA junction at different biases

After applying a constant bias, the gap distance slowly changes. H-bonds of established 4-MBA/4-MBA junction can only be formed within a small range of gap distances. We compare the appearance time of the last *v*(C=O) mode peak in spectra, indicating the last h-bond formation event, in a 30-min time window after the bias application. As shown in Figure S8, only at zero bias, the h-bond formation event occurs in the full 30-min time window. The time duration to observe the last h-bond formation event is obviously reduced either at non-zero biases.

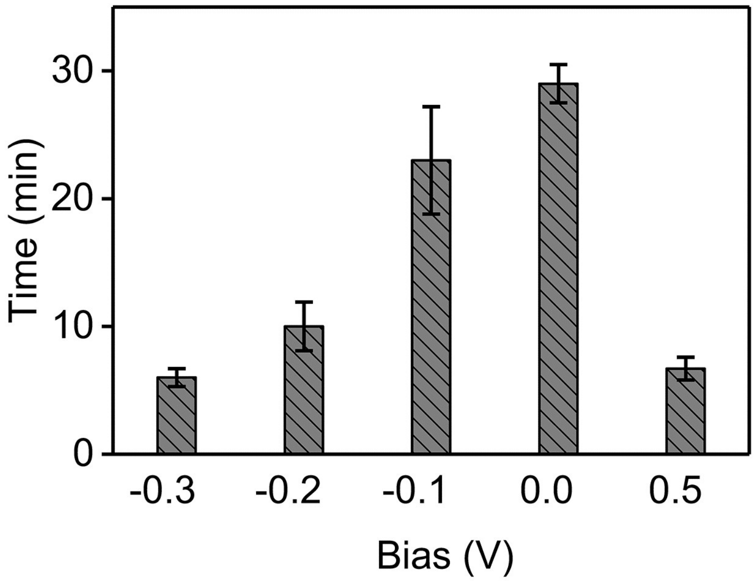

Figure S8. The time to observe the last appearance of *v*(C=O) mode peak in SERS spectra in 30-min time window, at -0.3 V, -0.2 V, -0.1 V, 0.0 V, +0.5 V respectively. The error bars are the standard deviation of at least 3 measurements. The solution is 5 mM PBS with 3 mM $K_4Fe(CN)_6$.

S7. The simultaneous SERS and electrochemical current change signals from established GNE-4-MBA/4-MBA-GNP junctions

We have studied the simultaneous responses of SERS and electrochemical (EC) current signals of GNE/4-MBA/4-MBA/GNP junctions at +0.5 V bias in 5 mM PBS with the redox mediator ($Fe(CN)_6^{4-}$). The setup has the sensitivity to detect a current change about 1 pA with a temporal resolution better than 1 ms. In order to observe clear current changes, the concentration of $Fe(CN)_6^{4-}$ is increased to 20 mM. It should be noted that the charging current is too small to be observed in our system.[1] Figure S9a shows the typical EC current change signals during “hit-stay-run” and “hit-n-stay” events.

No EC current change signals are observed in “hit-stay-run” events with the presence of GNPs in the solution (see trace i in Figure S9a). However, upward current spikes are observed from time to time after the molecular junctions are established by adsorbed GNPs (see traces ii-iv in Figure S9a). In the established 4-MBA/4-MBA junctions, the interfacial interactions are generally stronger, leading to the reduced electrical resistance and thus observable current change signals.

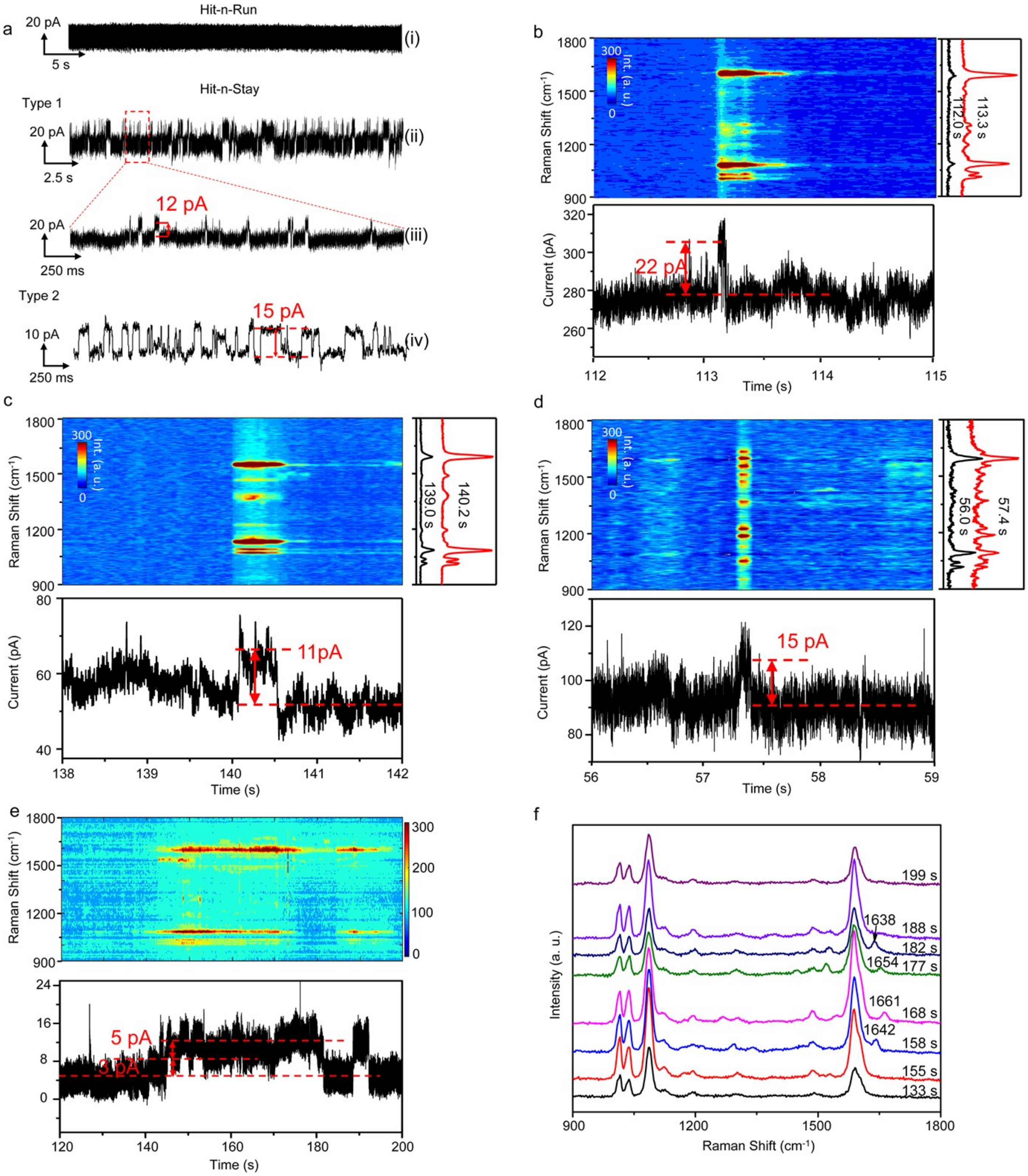

Figure S9. (a) Typical *I-t* traces. b-e) SERS and EC current transient changes with no GNPs in solution. The constant backgrounds (the black color spectra at the right-side) in these SERS trajectories have been subtracted. (f) SERS spectra at different time in the SERS trajectory (e). The background spectrum (*i.e.*, the spectra at 133 s) has not been subtracted from these spectra. All the curves and spectra are collected at +0.5 V in 5 mM PBS with pH = 7.4. The redox mediator ($Fe(CN)_6^{4-}$) concentration is 20 mM.

The spike height varies from several pA to several 10s of pA but is mostly around 10-20 pA. These current spikes indicate the transient increase of pair junction conductance. The origin of these upward current spikes likely comes from the transient formed new interactions and the stochastic movement of gold atoms in the nanogap or the overall movement of the adsorbed GNP.

Sometimes, simultaneous changes can be observed in both current and Raman signals. The examples are shown in Figure s9 b-f. To focus on the transient spectral change, the constant background (the black color spectrum shown at the right side inset) has been subtracted from these SERS trajectories. As shown in Figures S8 b-d. The Raman intensity suddenly increases, which is attributed to the small motion of adsorbed GNP (b-c) or the motion of a surface gold aom (d). The multiple new peaks in the SERS trajectory of Figure S9d are likely the signature of a 'picocavity' due to the very high local electromagnetic field.[11] A current spike also appears at the same time. The duration time of current change and SERS signal change is not always the same. The durations of current spikes are typically shorter, which is attributed to the higher distance sensitivity of tunneling current than that of SERS signal.[1] The establishment of intermolecular interaction is signaled by the appearance of two b2 mode peaks at 1003 cm^{-1} and 1027 cm^{-1} of 4-MBA. Both asymmetric b2 peaks are always observed when current spikes appear. Therefore, the intermolecular interactions should improve the electronic coupling at the intermolecular interface and contribute to the improved junction conductance.

In Figure s9e, the sudden increase of Raman intensity lasts for a much longer time. This type of signal was only observed shortly (~ 3 mins in this case) after applying +0.5 V to the GNE. The current also increases correspondingly. Several snapshots of the Raman spectra are shown in Figure s9f. The appearance of three b2 mode peaks at 1003 cm^{-1}, 1027 cm^{-1} and 8b suggests the formation of intermolecular h-bonds. The appearance of additional ν(C=O) peak around 1661 cm^{-1} suggests the formation of enhanced h-bond during the 'on time. The formation of enhanced h-bond can also explain the extended 'on' time of this event. The roughly two-level fluctuation of 'on' current may reflect the two different h-bond states. It should be mentioned that the lifetime of ν(C=O) peak is generally shorter and the ν(COO^-) peak does not appear in the solution with increased ionic strength. These differences suggest the strength of enhanced h-bond in established 4-MBA/4-MBA junction is weakened in solution with a relatively high ionic strength.

REFERENCES

1. J. Guo, J. Pan, S. Chang, X. Wang, N. Kong, W. Yang and J. He, *Small*, 2018, DOI: doi:10.1002/smll.201704164, 1704164.
2. G. Lu, B. Shrestha and A. J. Haes, *The Journal of Physical Chemistry C*, 2016, **120**, 20759-20767.
3. N. Marom, A. Tkatchenko, M. Rossi, V. V. Gobre, O. Hod, M. Scheffler and L. Kronik, *Journal of Chemical Theory and Computation*, 2011, **7**, 3944-3951.
4. S. Kristyán and P. Pulay, *Chem. Phys. Lett.*, 1994, **229**, 175-180.
5. X. Zhang, Z. Yu, W. Ji, H. Sui, Q. Cong, X. Wang and B. Zhao, *J. Phys. Chem. C*, 2015, **119**, 22439-22444.

6. H. Y. Jung, Y.-K. Park, S. Park and S. K. Kim, *Anal. Chim. Acta*, 2007, **602**, 236-243.
7. S. B. Lee, K. Kim and M. S. Kim, *Journal of Raman Spectroscopy*, 1991, **22**, 811-817.
8. Y. Fleger, Y. Mastai, M. Rosenbluh and D. H. Dressler, *Surf. Sci.*, 2009, **603**, 788-793.
9. M. Osawa, N. Matsuda, K. Yoshii and I. Uchida, *J. Phys. Chem.*, 1994, **98**, 12702-12707.
10. S. W. Bishnoi, C. J. Rozell, C. S. Levin, M. K. Gheith, B. R. Johnson, D. H. Johnson and N. J. Halas, *Nano Lett.*, 2006, **6**, 1687-1692.
11. F. Benz, M. K. Schmidt, A. Dreismann, R. Chikkaraddy, Y. Zhang, A. Demetriadou, C. Carnegie, H. Ohadi, B. de Nijs, R. Esteban, J. Aizpurua and J. J. Baumberg, *Science*, 2016, **354**, 726.